BMC Microbiology

RESEARCH Open Access

EsxA, a type VII secretion system-dependent effector, reveals a novel function in the sporulation of *Bacillus cereus* ATCC14579

Harvey K. Kamboyi[1], Atmika Paudel[1,2], Misheck Shawa[1,3], Misa Sugawara[1], Tuvshinzaya Zorigt[1], Joseph Y. Chizimu[4,5], Tomoe Kitao[1], Yoshikazu Furuta[1], Bernard M. Hang'ombe[6], Musso Munyeme[7] and Hideaki Higashi[1*]

Abstract

Background *Bacillus cereus* is a Gram-positive, spore-forming bacterium that produces a spectrum of effectors integral to bacterial niche adaptation and the development of various infections. Among those is EsxA, whose secretion depends on the EssC component of the type VII secretion system (T7SS). EsxA's roles within the bacterial cell are poorly understood, although postulations indicate that it may be involved in sporulation. However, the T7SS repertoire in *B. cereus* has not been reported, and its functions are unestablished.

Methods We used the type strain, *B. cereus* ATCC14579, to generate *ΔessC* mutant through homologous recombination using the homing endonuclease I-SceI mediated markerless gene replacement. Comparatively, we analyzed the culture supernatant of type strain and the *ΔessC* mutant through Liquid chromatography-tandem mass spectrometry (LC-MS/MS). We further generated T7SSb-specific gene mutations to explore the housekeeping roles of the T7SSb-dependent effectors. The sporulation process of *B. cereus* ATCC14579 and its mutants was observed microscopically through the classic Schaeffer-Fulton staining method. The spore viability of each strain in this study was established by enumerating the colony-forming units on LB agar.

Results Through LC-MS/MS, we identified a pair of nearly identical (94%) effector proteins named EsxA belonging to the *sag*EsxA-like subfamily of the WXG100 protein superfamily in the culture supernatant of the wild type and none in the *ΔessC* mutant. Homology analysis of the T7SSb gene cluster among *B. cereus* strains revealed diversity from the 3' end of *essC*, encoding additional substrates. Deletions in *esxA1* and *esxA2* neither altered cellular morphology nor growth rate, but the *ΔesxA1ΔesxA2* deletion resulted in significantly fewer viable spores and an overall slower sporulation process. Within 24 h culture, more than 80% of wild-type cells formed endospores compared to less than 5% in the *ΔesxA1ΔesxA2* mutant. The maximum spore ratios for the wild type and *ΔesxA1ΔesxA2* were 0.96 and 0.72, respectively. Altogether, these results indicated that EsxA1 and EsxA2 work cooperatively and are required for sporulation in *B. cereus* ATCC14567.

*Correspondence:
Hideaki Higashi
hidea-hi@czc.hokudai.ac.jp

Full list of author information is available at the end of the article

Conclusion *B. cereus* ATCC14579 possesses two nearly identical T7SSb-dependent effectors belonging to the *sag*EsxA-like proteins. Simultaneous deletion of genes encoding these effectors significantly delayed and reduced sporulation, a novel finding for EsxA.

Keywords *Bacillus cereus*, Type VIIb secretion system, EsxA, Sporulation

Introduction

Bacillus cereus, a Gram-positive, spore-forming bacterium belonging to the Firmicutes phylum, has been primarily associated with food poisoning. But recently, some strains have been implicated in severe infection, including bacteremia [1, 2], while others have evolved to produce lethal anthrax-like disease [3]. *B. cereus* has been considered a neglected pathogen, but studies are now unraveling the evolution of its virulence mechanisms. The ability to express a variety of virulence factors, including pore-forming toxins, hemolysins, enterotoxins, proteases, and phospholipases, is central to its ability to cause infections in humans and animals as well as colonizing the environment [4].

Among the Firmicutes bacterial mechanisms that facilitate their virulence is the secretion system for the passage of toxigenic materials. Like other Gram-positive bacteria, *B. cereus* is expected to have a type VII secretion system (T7SS) possessing a specialized transmembrane nanomachinery, EssC, belonging to the FtsK/SpoIIIE ATPase protein family. The T7SS was first discovered in *Mycobacterium tuberculosis* [5], and recent studies on Gram-positive bacteria have shown limited homology to the mycobacterial T7SS components, which led to the sub-classification of T7SS into T7SSa (Actinobacteria) and T7SSb (Firmicutes) [6, 7]. Despite a limited structural similarity, T7SS share highly similar substrates, including the early secretory antigenic targets (ESAT) A (EsxA) and B (EsxB), containing a conserved Trp–Xaa–Gly (WXG) central sequence motif. EsxA and EsxB are small acidic proteins of the WXG100 superfamily, which have shown to be strong cytotoxic T-cell antigens [8, 9] and possess pore-forming activity [10]. EsxA alone or in combination with EsxB causes dose-dependent pore-formation in host cell membranes, which could be crucial for the translocation of other bacterial virulence factors into the host [10, 11]. Recently, studies in *Staphylococcus aureus* have shown that secretion of these effector proteins requires a functional EssC [7, 12]. Studies have also established that EsxB alone binds via its C-terminal secretion signal sequence to an empty pocket on the EssC C-terminal, accompanied by an increase in ATPase activity. Surprisingly, substrate binding does not activate EssC allosterically but by stimulating its multimerization, forming a hexameric pore necessary for the secretion of T7SS-dependent effectors [13]. These findings suggest that WXG100 proteins are virulence factors outside the cell and may have other housekeeping roles since they are also found among non-pathogenic organisms [14, 15].

Further, T7SS genes encoding additional WXG100-like effectors, EsxC and EsxD, have been identified in *S. aureus*, and the polymorphic LXG toxin among Firmicutes and their functions have been characterized (Fig. 1) [8, 16, 17]. The TIGR04197 proteins have recently been remotely linked to the T7SS based on phylogenetic profiling as a putative T7SS effector. In addition, a site-specific mutation in the TIGR04197 encoding gene abrogated LXG effector export, suggesting its significance in LXG effector secretion by the T7SSb apparatus in *Streptococcus intermedius* [18]. Despite many studies on T7SS in various species of medical importance, the repertoire of the secretion system in *B. cereus* has not been reported and is always inferred from other Firmicutes members. Among the closely related *Bacillus* species, the T7SS has been established in *B. subtilis* (Fig. 1) [19, 20] and *B. anthracis* [21].

Like EssC, SpoIIIE belongs to the FtsK/SpoIIIE ATPase protein family, but it is indispensable for DNA translocation from the mother cell to the apically located forespore during sporulation [22]. *B. cereus* possesses both EssC and SpoIIIE for the T7SSb and spore formation, respectively. SpoIIIE acts as a checkpoint that prevents septal membrane fusion until the completion of chromosome translocation via the aqueous DNA-conducting hexameric pole. Both proteins are multidomain with high homology in the substrate-binding C-terminal motor domain, and recruitment of multiple factors precedes multimerization [13, 23, 24]. However, it is unknown whether an EssC substrate can bind to another FtsK/SpoIIIE protein, such as SpoIIIE, and affect its function(s).

Therefore, this study first sought to identify the T7SSb-dependent effectors and establish the T7SSb gene locus in *B. cereus.* Relying on data from the well-studied T7SSb in *S. aureus* USA300, we generated a *B. cereus* ATCC14579 *ΔessC* mutant to identify T7SSb-dependent effectors. Here, we performed a comprehensive proteomic analysis of the culture supernatant for *B. cereus* ATCC14579 and its *ΔessC* mutant and identified two nearly identical EsxA proteins, EsxA1 and EsxA2. Secondly, we explored the influence of the identified effectors in the phenotypic characteristics of *B. cereus* ATCC14579 after generating single and double mutations for the T7SSb effectors genes. We established that *B. cereus* ATCC14579

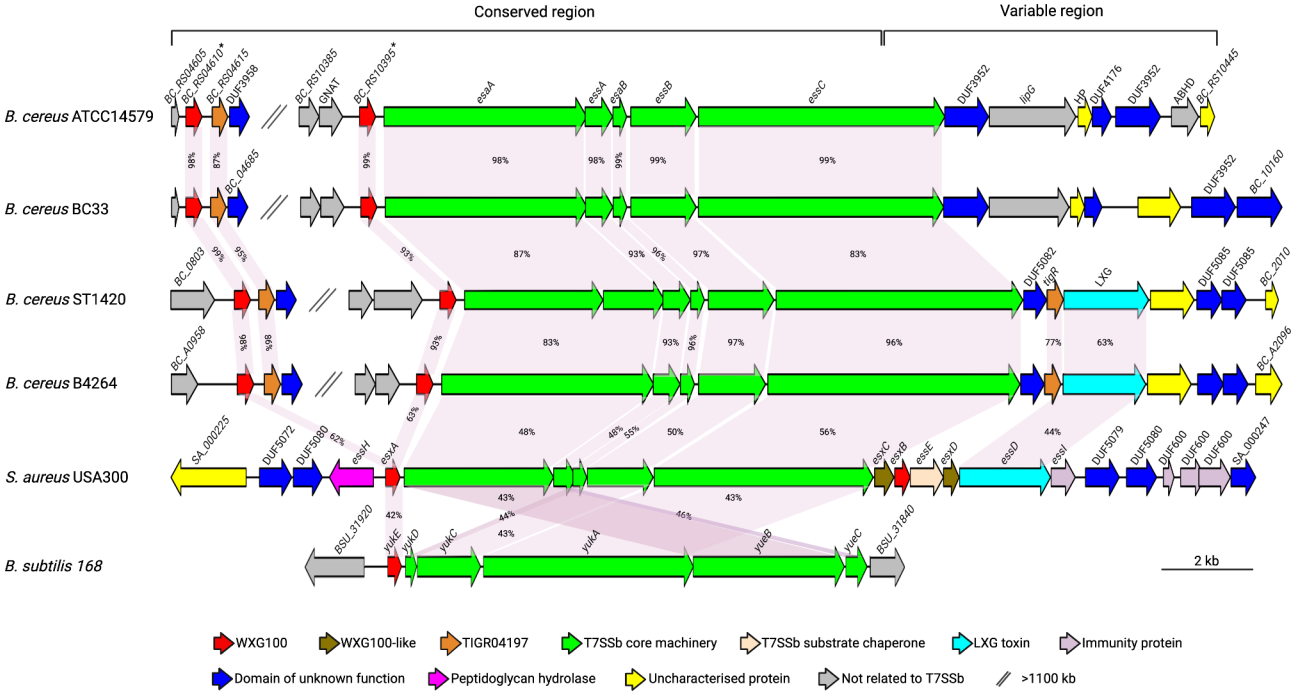

Fig. 1 Schematic representation of the T7SSb gene cluster in *B. cereus* ATCC14579 (GenBank: NC_004722.1). The putative WXG100 protein-encoding genes, *BC_RS04610* and *BC_RS10395*, are indicated with asterisks. Homology analysis of the corresponding T7SSb gene clusters in different *B. cereus* strains *S. aureus* USA300 and *B. subtilis* 168 are also shown. The same color indicates related genes, and percentage identities for each gene, with reference to *B. cereus* ATCC14579, are shown in pink-shaded areas. Genes at the 5′ end of the *essC* are highly conserved, while variation is observed in the 3′ end

ΔesxA1ΔesxA2 displayed a significantly decreased sporulation phenotype compared to the wild type.

Materials and methods

Bacterial strains and growth conditions

For routine culture, *B. cereus* strains were grown in Brain Heart Infusion (BHI) medium (Difco, USA) at 37 °C (shaking at 155 rpm for liquid cultures) and *Escherichia coli* strains in Luria-Bertani (LB) medium (Difco, USA). The bacterial strains and plasmids used in this study are shown in Table 1. Cultures for protein mass spectrometry were done in minimal medium (M9), 2% glucose, 50 mM Na_2HPO_4, 25 mM KH_2PO_4, 10 mM NaCl, 20 mM NH_4Cl, 1 mM $MgSO_4{\cdot}7H_2O$, 0.1 mM $CaCl_2$, 10 mM glutamic acid, 1.4 mM threonine, 0.6 mM leucine, 2.5 mM valine, 1.4 mM histidine and 0.3 mM methionine at 37 °C. When needed, antibiotics were added to LB at final concentrations of 250 µg/ml (*B. cereus*) or 100 µg/ml (*E. coli*) spectinomycin, 60 units/ml polymyxin, 50 µg/ml kanamycin, and 100 µg/ml ampicillin. For sporulation assays, we used 0.8% Nutrient Broth (Difco, USA), 1.2% (w/v) $MgSO_4{\cdot}7H_2O$, 10% (w/v) KCl, 1 mM $Ca(NO_3)_2$, 0.01 mM $MnCl_2{\cdot}6H_2O$, and 1 µM $FeSO_4{\cdot}7H_2O$ (pH=7.6) [25] under aerobic conditions at 30 °C with shaking at 200 rpm.

Construction of plasmids and gene knockout procedure

To construct the *essC*-knockout mutant strain, the upstream (US) and downstream (DS) homologous arms of *B. cereus* ATCC14579 were inserted into plasmid pRP1028 between the *BanII-SacI* and *BsaI* sites to construct the pYF07. The US and DS fragments were generated via PCR using the primers indicated in Table 2. PCR and sanger sequencing further verified the resulting plasmids using appropriate primers. The same procedure was used to construct pHKK100, pHKK102, and pHKK104 plasmids. The allelic exchange system used in this study was developed based on the homing endonuclease I-SceI mediated markerless gene replacement method established in *B. anthracis* [26] with minor variations. We used the biparental mating method, eliminating the use of the helper strain (*E. coli* SS1827). We used *E. coli* SM10 and S17-1, which have *tra* genes encoding factors that can mobilize *oriT*-containing plasmids and integrate into chromosomes, thus making biparental mating possible. *E. coli* SM10 was used for pRP1028 derivatives conjugative transfer, and *E. coli* S17-1 was used to transfer pRP1099. Confirmation of gene deletion was done using PCR and sanger sequencing. This allelic exchange procedure is illustrated in Figure S1. The same method was used to create *ΔesxA1*, *ΔesxA2*, *and ΔtigR* mutants of *B. cereus* ATCC14579. To construct the double mutant, we used *B. cereus ΔesxA1* and *E. coli* SM10 harboring

Table 1 Strains and plasmids used in this study

Strain	Genotype or Description	Source
B. cereus		
ATCC14579	Wild type	[28]
	ΔessC (*essC* gene deleted mutant)	This study
	ΔesxA1 (*esxA1* gene deleted mutant)	This study
	ΔesxA2 (*esxA2* gene deleted mutant)	This study
	ΔtigR (*tigR* gene deleted mutant)	This study
	ΔesxA1ΔesxA2 (*esxA1* and *esxA2* genes deleted mutant)	This study
	ΔesxA1ΔesxA2 + pGFP78::*esxA1* (*ΔesxA1ΔesxA2* mutant complimented with its native *esxA1* gene)	This study
	ΔesxA1ΔesxA2 + pGFP78::*esxA2* (*ΔesxA1ΔesxA2* mutant complimented with its native *esxA2* gene)	This study
	ΔesxA1ΔesxA2 + pGFP78 (*ΔesxA1ΔesxA2* mutant complimented with pGFP78 plasmid)	This study
	Wild type + pGFP78 (Wild type complimented with pGFP78 plasmid)	This study
E. coli		
SM10	*thi thr leu tonA lacY supE recA::RP4-2-Tc::Mu (Km)*	[29]
S17-1	*thi, pro, hsdR, RP4-2 Tc::Mu Km::Tn7 (Tp Sm)*	[29]
DH10β (C3019H)	*Δ(ara-leu) 7697 araD139 fhuA ΔlacX74 galK16 galE15 e14- Φ80dlacZΔM15 recA1 relA1 endA1 nupG rpsL (StrR) rph spoT1 Δ(mrr-hsdRMS-mcrBC)*	New England BioLabs
Plasmids		
pRP1028	*Bacillus* and *E. coli* shuttle vector with *turbo-rfp* gene and an I-SceI recognition site; Spe^R	[26]
pRP1099	Vector with *turbo-AmCyan* and I-SceI genes; Kan^R	[26]
pGFP78	Shuttle vector for *Bacillus* and *E. coli* containing *gfp* gene and F78 promoter; Amp^R, Tet^R	[27]
pYF07	pRP1028 with upstream and downstream regions of *essC*	This study
pHKK100	pRP1028 with upstream and downstream regions of *esxA1*	This study
pHKK102	pRP1028 with upstream and downstream regions of *esxA2*	This study
pHKK104	pRP1028 with upstream and downstream regions of *tigR*	This study
pHKK114	pGFP78 *Δgfp* with *esxA1*	This study
pHKK115	pGFP78 *Δgfp* with *esxA2*	This study

SpeR, KanR, TetR, and AmpR stand for spectinomycin, kanamycin, tetracycline, and ampicillin resistance, respectively

pHKK102 and followed the same allelic exchange procedure from step 4 (Fig. S1).

Construction of complimentary strains

To complement the *B. cereus ΔesxA1ΔesxA2* mutation, a *GFP* plasmid, pGFP78, an *Escherichia coli–Bacillus subtilis* shuttle vector carrying a constitutive 78 promoter-controlled *GFP* gene was used. The GFP open reading frame was removed from this vector by digestion with XbaI and HindIII [27]. *B. cereus* ATCC14579 genome was used to amplify *esxA1* and *esxA2* using specific primers in Table 2, and each was ligated to the XbaI and HindIII sites of the linearized plasmid to generate each respective complementation plasmid. The orientation and sequence of PCR fragments were confirmed by sanger sequencing. The recombinant plasmids were each electroporated into *B. cereus ΔesxA1ΔesxA2* producing *B. cereus ΔesxA1ΔesxA2*+pGFP78::*esxA1 and B. cereus ΔesxA1ΔesxA2*+pGFP78::*esxA2* mutants. Successful transformants were selected on LB agar plates supplemented with 10 µg/ml tetracycline and further confirmation by sanger sequencing. In addition, we complemented *B. cereus* ATCC14579 and the *ΔesxA1ΔesxA2* mutant with pGFP78 for growth in tetracycline. All strains constructed in this study are listed in Table 1.

Liquid chromatography-tandem mass spectrometry

B. cereus ATCC14579 and its *ΔessC* mutant were each grown in 2.5 ml LB at 37 °C for 18 h, and then cells were pelleted and washed three times in M9. Resuspended cells were incubated in M9 with start OD_{600}=0.05 at 37 °C until mid-log phase (~5 h). The cells were pelleted and filtered the culture supernatant using a 0.45 µm membrane filter (Millipore, Ireland). The supernatant was purified using methanol-based C8 reverse-phase liquid chromatography (Strata™ Phenomenex, USA). The purified protein mixture then underwent alkylation, tryptic digestion, and further peptide purification using Pierce™ C18 spin columns (ThermoFisher Scientific, USA) following the manufacturer's protocol. The peptide mixtures were analyzed using the HPLC liquid phase system EASY nLC1000 (ThermoFisher Scientific, USA). They were loaded onto a C18 column (3 µm particle diameter, 0.075 mm x 120 mm, Nikkyo Technos, Japan) at a 300 nl/min flow rate controlled by intelliflow technology over 81 min. The HPLC was coupled online via a nanoelectrospray ion source to a hybrid ion trap

Table 2 Primers used in this study

Primer name	Sequence (5′–3′)[a]	Application
*essC*_US_F	cttgagctcctagcggccgcaagaaatgagaaattaagactacttcgg	For construction of *ΔessC mutant*
*essC*_US_R	ttaatttcagaattccatccgtgttcactgctc	
*essC*_DS_F	acacggatggaattctgaaattaaagaagaaagctaaggtg	
*essC*_DS_R	gtacaggtctccggccgctctgcgttaaatttatcctgtaatgtc	
*esxA1*_US_F	tcctagcgatgtgtgactatattggctgtttttatccaga	For construction of *ΔesxA1 mutant*
*esxA1*_US_R	gtatgacaatttttttcatttccccttttaatacataatgagcaaaatataaattgg	
*esxA1*_DS_F	gggaaatgaaaaaattgtcatactctatataacaagcatttcaaatgagc	
*esxA*_1_DS_R	tctccggccttaacttttgatttacttgattgatttgtttttcaatatcttgact	
*esxA2*_US_F	gcttgagcggatggatattaataggggaaaatacagactatttttct	For construction of *ΔesxA2 mutant*
*esxA2*_US_R	ctttttatctgtctattaaatccccctttaaaattaaaaaatagtaaaattaaccaataatca	
*esxA2*_DS_F	ggggatttaatagacagataaaaagaaatatataatttagccatgcaacc	
*esxA2*_DS_R	cgctaggattctgcctcagctttcaaatcct	
*tigR*_US_F	agcttgagcgttagtttggctgtagtagatattatcgttgcgaat	For construction of *ΔtigR mutant*
*tigR*_US_R	ggttgtcacacactcaaatcctttctctaattttcagaacatg	
*tigR*_DS_F	atttgagtgtgtgacaacctacgtaaaggtaaaatagtaagagga	
*tigR*_DS_R	gccgctaggactaatatttcttgttcaattacatctgtggaagc	
Dx_*esxA1*_F	ccaatttatattttgctcattatgtattaaagggg	PCR and sanger sequencing confirmation of *esxA1* deletion
Dx_*esxA1*_R	ctttgaaattgtcccatcactcaaatcctttctc	
Dx_*tigR*_F	ggctcatttgattgcatgcccaac	PCR and sanger sequencing confirmation of *tigR* deletion
Dx_*tigR*_R	cctgaatgtgaatcgcggattgatttcggtc	
Dx_*esxA2*_F	ggtttgcctttattttatagtagatttatagagtgtgc	PCR and sanger sequencing confirmation of *esxA2* deletion
Dx_*esxA2*_R	cgactgcgagtctatctaatgaaagacttcgtatc	
*esxA1*_F_C	gc*tctaga*caatttatattttgctcattatgtattaaagggg	For construction of *esxA1* complimentary strain
*esxA1*_R_C	ccc*aagctt*gctcatttgaaatgcttgttatatagagtatgac	
*esxA2*_F_C	gc*tctaga*ggtttgccttattttatagtagatttatagagtgtgc	For construction of *esxA2* complimentary strain
*esxA2*_R_C	ccc*aagctt*cgactgcgagtctatctaatgaaagacttcg	

[a] Restriction sites are italicised

quadrupole-Orbitrap (LTQ–OrbitrapXL; ThermoFisher Scientific) tandem mass spectrometer (LC-MS/MS) [30]. The LC−MS/MS.RAW files were searched against *B. cereus* ATCC 14,579 protein FASTA file database and annotated the peptides using the Sequest HT algorithm in Proteome Discoverer 1.4.1.14 (DBVersion:79) (Thermo Fisher Scientific, Waltham, MA). The reference strain *B. cereus* BC33 (GenBank: CP072774.1) was also used as a database to validate the peptide annotations from the *B. cereus* ATCC14579 database. Search parameters were set to two missed trypsin cleavage sites, and a precursor mass tolerance of 10 ppm and a fragment mass tolerance of 0.06 Da were utilized. The search included carbamidomethylation of cysteine as a static modification and amine carbamylation and methionine oxidation as dynamic modifications, with a maximum of four modifications per peptide. The false discovery rate for peptide-spectrum matches (PSMs) was set at 1% maximum using a target-decoy PSM validator [31, 32].

B. cereus T7SSb-dependent effectors and gene cluster

Sequences of annotated proteins in the mass spectrometry data were obtained from the GenBank files and analyzed for motifs found among known T7SS substrates using the GenomeNet platform [33] to validate their identity. Further bioinformatic searches were conducted using web resources NCBI BLASTp [34] (available at https://blast.ncbi.nlm.nih.gov/Blast.cgi) to obtain the best hits among Firmicutes for CLUSTAL O alignment. Furthermore, genes encoding the candidate T7SSb effectors were obtained for homology and neighborhood analysis against the well-studied and established T7SSb in *S. aureus* USA300 (GenBank: CP092052.1) and *B. subtilis* 168 (GenBank: AL009126.3). This analysis was used to identify the T7SSb core machinery encoding genes, and the output data was imported into genoPlotR [35] to construct the gene cluster. Additionally, a comparative analysis of genome sequences was performed to detect T7SSb in the reference strain, *B. cereus* BC33 (GenBank: CP072774.1), and the more virulent strains, *B. cereus* ST1420 (GenBank: AP022975.1) and *B. cereus* B4264 (GenBank: CP001176.1). CLUSTAL O version 1.2.4 multiple sequence alignment was used to calculate the T7SSb nucleotide sequence similarity among the selected strains.

Growth curve measurements

Our proteogenomic analysis identified two T7SSb-dependent effectors designated EsxA1 and EsxA2 and one T7SS target, TIGR04197, although it was not found

in the culture supernatant. Therefore, we further generated *ΔesxA1*, *ΔesxA2*, *ΔesxA1ΔesxA2 and ΔtigR* strains in addition to *ΔessC* for further analysis. Bacterial cultures were prepared in BHI for 18 h and then diluted to OD_{600}=0.1. Ten technical replicates of diluted culture for each strain were added to the 96-well plate and monitored for growth by measuring OD_{600} every 10 min for 10 h using the Varioskan LUX Multimode Microplate Reader (Thermo Scientific, USA) at 37 °C while shaking at 600 rpm. Growth rates were estimated from the slopes (log phase) obtained by fitting parametric models to the resulting data using GraphPad Prism version 8.4.3. This experiment was also done in LB and DSM cultures and done in three biological replicates.

Determination of sporulation

The sporulation process observed under aerobic conditions in DSM has been shown to induce stronger sporulation capabilities in *B. cereus* [36]. *B. cereus* ATCC14579 and its five mutants were grown at 37 °C in LB for 18 h and then diluted to OD_{600}=0.1 in 10 ml DSM. The DSM culture was incubated under aerobic conditions at 30 °C overnight with shaking at 200 rpm and then upscaled to 100 ml for up to 166 h until the fraction of spores/vegetative cells reached a maximum level [36]. One milliliter of aliquots of each sample was obtained every 12 h for measuring the OD and every 24 h for establishing the colony forming units (CFU) per ml. Serial dilutions of 100 µl culture and 900 µl of 1 × phosphate buffered saline up to 10^6 dilutions were made. From the 10^6 dilutions, an aliquot of 500 µl was heat-treated at 80 °C for 10 min to kill vegetative cells in the culture and then immediately put on ice [37, 38] while the other 500 µl remained untreated. Four 20 µl replicates of heat-treated and untreated aliquots were plated on LB and then incubated at 28 °C for 14 h to enumerate the CFUs. Complementation experiments were done in DSM supplemented with 10 µg/ml tetracycline. The mean CFU and sporulation ratios were obtained by CFU/ml=mean CFU ÷ (ml plated × dilution factor) and sporulation ratio=heat-treated mean CFU/ml ÷ untreated mean CFU/ml, respectively. Part of the undiluted daily aliquots were stained using the classical Schaeffer-Fulton staining method [39]. The slides were viewed by phase-contrast microscopy (×100, oil immersion; Nikon ELIPSE Ti, Nikon, Japan) with at least three visual fields examined to calculate the sporulation rate and images taken using a Nikon COOLPIX P310 camera. Sporulation rate = [mean spore count ÷ (mean spore count+mean vegetative cell count)] × 100%.

Statistical analyses

The statistical tests were performed using GraphPad Prism 8.4.3, as indicated in the figure legends, with *P* values<0.05 considered significant. An ordinary unmatched one-way analysis of variance (ANOVA) with Dunnett's multiple comparisons test was applied for OD computations, and CFU counts for the same time point. A matched two-way ANOVA was used for growth kinetics, daily OD, and sporulation ratio. All experiments were conducted with at least three biological and four technical replicates.

Results

Organization and characteristics of T7SSb gene cluster in *B. cereus*

Gene neighborhood analysis identified candidates for the T7SSb locus in *B. cereus* ATCC14579 (Fig. 1). In addition, the *S. aureus* USA300 [12, 16] and *B. subtilis* 168 T7SS [20] nucleotide sequence homology analysis led to the identification of the genetic organization of T7SSb in *B. cereus* with notable differences. *B. cereus* ATCC14579 possesses two copies of the putative WXG100 protein-encoding genes locus tagged *BC_RS04610* and *BC_RS10395*. *BC_RS04610* is located>1100 kb upstream of *BC_RS10395*, and the latter is immediately upstream of the T7SS core machinery genes. Immediately downstream of *BC_RS04610* is the *BC_RS04615*, encoding a putative T7SS effector of the TIGR04197 protein family. The TIGR04197 protein sequence has no known signal peptide, interactions, or function. However, our analysis did not find TIGR04197 in the *B. cereus* secretome, nonetheless, we included it in the preceding experiments. Additional analysis, which included other *B. cereus* strains, showed that the T7SSb gene cluster is conserved up to 5' two-thirds of the *essC* encoding the ATPase domain indispensable for secretion of T7SSb-dependent effectors. One-third on the 3' end of *essC* and the ensuing genes within the T7SSb cluster showed variation among the less virulent *B. cereus* ATCC14579 and *B. cereus* BC33. The clinical isolates, *B. cereus* ST1420 and *B. cereus* B4264, possess a second TIGR04197 protein and LXG toxin genes within the cluster. In contrast, the variable region in *S. aureus* encodes other T7SSb effectors, EsxB, EsxC, EsxD, and LXG toxin, including immunity proteins (Fig. 1). LXG toxins are diverse and polymorphic, with N-terminal LXG delivery domains and diverse C-terminal toxin domains that mediate intercellular competition in biofilms via the T7SS in *S. aureus* and *B. subtilis* [40, 41].

Identification of T7SSb-dependent effectors

To identify the *B. cereus* T7SSb-dependent effector proteins, first, we generated the *ΔessC* mutant using *B. cereus* ATCC14579. The mid-log phase M9 culture of *B. cereus* ATCC14579 (wild type) and its *ΔessC* mutant were utilized in the secretome analyses to identify the T7SSb-dependent effectors. From the LC-MS/MS raw data, the search algorithm in Proteome Discoverer identified 92

proteins in the wild type (WT) and 77 proteins in the *ΔessC* mutant on average for three independent experiments. To increase confidence in the identifications, we limited our analysis to those proteins identified by two or more peptides. Of the 92 proteins in the secretome of wild type, only two were annotated as ESAT-6-like [*Bacillus cereus*] (Table S1). Motif search analysis of the secretomes in GenomeNet confirmed the two proteins designated Q81HA0 and Q81EA6 were related to T7SS. The two ESAT-6-like proteins had 94% sequence identity and were found in the WT secretome, but none in *ΔessC* (Fig. 2A). Proteins that did not possess known motifs related to the T7SS were excluded from further analyses. NCBI BLASTp search filtered for species diversity showed that the results comprised only firmicutes in the top 10 hits. CLUSTAL O multiple sequence alignments showed that they possessed a conserved centrally located WXG motif and C-terminal WXG100 secretion signal, *HxxxD/ExxhxxxH* (Fig. 2B). In addition, they had non-hydrophobic inter-dimer interacting residues at positions 21 and 39, confirming that the two effector proteins and those in the NCBI BLASTp results belong to the monocistronic expressed *sag*EsxA-like subfamily of the WXG100 protein superfamily [42, 43]. The proteins Q81HA0 and Q81EA6 were henceforth renamed EsxA1 and EsxA2, respectively. We confirmed that Q81HA0 and Q81EA6 were encoded in genes *BC_RS04610* and *BC_RS10395*, respectively.

Colony characteristics and growth patterns under normal conditions

The genes *BC_RS04610*, *BC_RS10395*, and *BC_RS04615* were renamed *esxA1*, *esxA2*, and *tigR*, respectively. We successfully generated *B. cereus* ATCC14579 full gene deletions in *esxA1*, *esxA2*, *esxA1esxA2*, and *tigR* in addition to *the ΔessC* mutant for further analyses. Some studies on the functional diversity of T7SS-dependent substrates have insinuated that secreted effectors may have multiple roles besides being just secreted virulence effectors [13, 44, 45]. Therefore, we screened the T7SSb mutant strains against the WT for morphotype changes and growth patterns' aberrations. When checked for colony characteristics, the WT and the mutant strains had similar colony size and morphology in BHI agar, and when plated on blood agar, they were all surrounded by a halo of hemolysis (Figs. S2A and S2B). Growth on cereus selective agar base supplemented with 100 units/ml polymyxin B and 5% egg-yolk emulsion (Merk, Germany), all strains induced egg-yolk precipitation with purple colonies and surrounding media (Fig. S2C). Simple linear regression of the log phase growth in minutes for all strains ($n=10$) in BHI (60–150), LB (70–150), and DSM (60–170) did not show any significant differences regardless of the media used. Since the slopes were not significantly different from each other, their pooled values of the log phases were 0.0058 ($R^2=0.995$), 0.0082 ($R^2=0.994$), and 0.0067 ($R^2=0.988$), in BHI, LB, and DSM, respectively. Thus, the gene deletions in this study

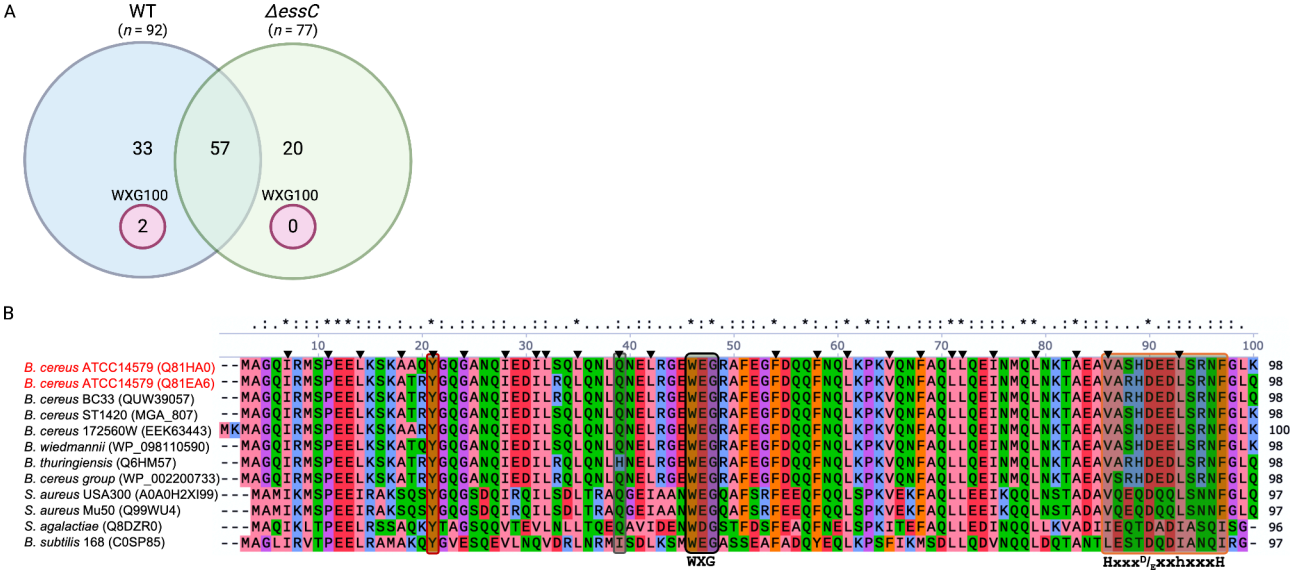

Fig. 2 WXG100 protein, *sag*EsxA-like, is conserved across T7SSb loci. **A.** Mid-log phase secretome analysis for *B cereus* ATCC14579 and its *ΔessC* mutant. Two WXG100 proteins were found in the WT and none in *ΔessC*. **B.** CLUSTAL O alignments of the two WXG100 protein sequences, Q81HA0 (EsxA1) and Q81EA6 (EsxA2), found in the WT secretome and other firmicutes species. The alignment shows the centrally located WXG motif and a conserved C-terminal secretion signal with the *HxxxD/ExxhxxxH*. In this sequence, 'H' stands for highly conserved hydrophobic and 'h' for less conserved hydrophobic residues, 'x' for any amino acid, and 'D/E' for either aspartic or glutamic acids, respectively. The four-helix bundle requires predominantly hydrophobic residues at a helix turn consisting of the heptad helix repeat shown by ▼ on the aligned residues. All residues involved in the inter-dimer interactions are hydrophobic except two residues, position 21 and 39, which are unique to the *sag*EsxA-like subfamily

did not alter the growth rate, suggesting T7SSb does not play a role in the growth of *B. cereus*. The growth curves and their respective simple linear regression log phase slopes are shown in (Fig. S3).

Growth under sporulation conditions was impaired in ΔesxA1ΔesxA2

Under normal growth conditions, the T7SSb mutants and the WT were indistinguishable; therefore, we next checked growth under nutritional stress conditions that stimulated sporulation. Growth in DSM was monitored by measuring OD_{600} every 12 h until a stable peak measurement. Figure 3A shows an exponential increase in OD in the first 36 h, followed by a sharp decrease in all strains except *ΔesxA1ΔesxA2* mutant, which exhibited a slow decline before becoming nearly constant after 120 h. At 120 h, *ΔesxA1ΔesxA2* had a significantly higher OD than other strains (Fig. 3B). The decrease in OD represented the sporulation process as mother cells lyse, releasing mature spores and shifting from the denser vegetative cells to smaller and lighter spores. Complementation of *esxA1esxA2* mutation with either *esxA1* or *esxA2* resulted in ODs comparable to the WT (Fig. 3C and D). The significantly higher OD in the *ΔesxA1ΔesxA2* mutant could be due to delayed autolysis by the mother cell required to release mature spores. In assessing this hypothesis, we recorded the spore ratio from CFUs and observed the sporulation rate microscopically recorded every 24 h. The highest CFU/ml for the untreated and heat-treated cultures was observed after 120 h, at which their ratio was maximal for all the strains. Extended cultures did not yield different results, thus, the CFU data presented

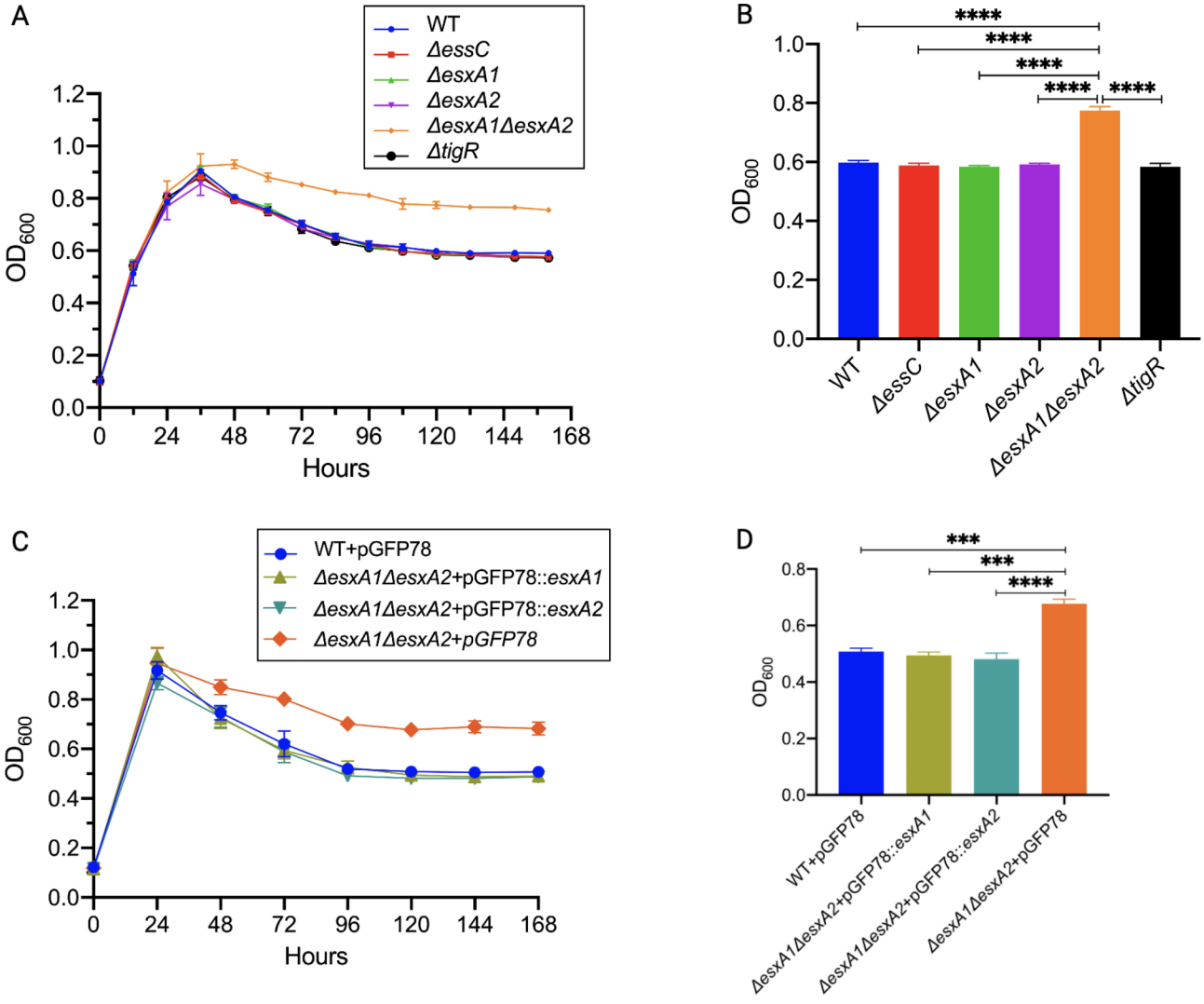

Fig. 3 Optical density measurement during culture in DSM at 30 °C. **A.** Optical density throughout the growth of *B. cereus* ATCC14579 and its mutants in DSM. **B.** Optical density measured after 120 h culture. **C**. Time-course and (**D**) at 120 h optical density for complemented strains. The results represent means ± SEM of 3 independent experiments. Statistical significance was calculated by Ordinary one-way ANOVA with Dunnett's test, $^{**}P = 0.002$; $^{***}P = 0.0003$ $^{***}P = 0.0002$; $^{****}P < 0.0001$

here were measured after 120 h of culture, which coincided with the stable OD (Fig. 4A). The *ΔesxA1ΔesxA2* mutant had a significantly lower spore ratio (~0.72), signifying fewer viable spores per ml. In contrast, *ΔesxA1*, *ΔesxA2*, *ΔessC and ΔtigR* mutants had spore ratio results comparable to the WT at all time points, peaking at approximately 0.96 (Fig. 4A). There was a significant reduction in the mean CFU/ml for the *ΔesxA1ΔesxA2* mutant when heat treated, indicating the presence of vegetative cells after 120 h (Fig. 4B and C). Such a reduction was not observed in the WT and other mutants. When complemented, maximum sporulation rates (97%) were restored in both *ΔesxA1ΔesxA2*+pGFP78::*esxA1* and *ΔesxA1ΔesxA2*+pGFP78::*esxA2* strains, demonstrating that *esxA1* and *esxA2* worked cooperatively and either was sufficient to restore the sporulation phenotype (Fig. 4D – F). Our findings indicated that EsxA was essential for optimum spore formation in *B. cereus* ATCC14579.

EsxA is essential for optimum sporulation in *B. cereus* ATCC14579

We found that the *ΔesxA1ΔesxA2* mutant had a significantly higher OD but a significantly lower CFU/ml, fewer spores, and a lower sporulation ratio. We conducted microscopy of the Schaeffer-Fulton method-stained cultures to evaluate our delayed mother cell autolysis hypothesis. Phase contrast microscopy showed early evidence of sporulation in the majority (>80%) of the WT cells generating endospores within 24 h compared to *ΔesxA1ΔesxA2* with less than 10%. The *ΔesxA1ΔesxA2* mutant endospores poorly took up malachite green stain at this time, suggesting fewer endospores (Fig. 5). After culturing for 48 h, WT released a mass of mature spores, but *ΔesxA1ΔesxA2* had a few mature spores, and almost 55% of the cells had endospores. Further, the *ΔesxA1ΔesxA2* mutant had vegetative cells beyond 96 h, which had maintained the typical chaining phenotype. The presence of vegetative cells accounted for the significantly higher OD and a reduced sporulation rate, whose peak was 72%. In contrast, at 96 h, the WT sporulation rate almost reached 100%. These findings ruled out our hypothesis, suggesting that delayed autolysis of mother cells with mature endospores caused a significantly higher OD and lower spore ratio, but rather, due to an inefficient sporulation process altogether. Again, complementation of *ΔesxA1ΔesxA2* with either *esxA1* or *esxA2* reversed the sporulation deficiency to levels of the WT (Fig. 6). Therefore, we concluded that the two EsxA

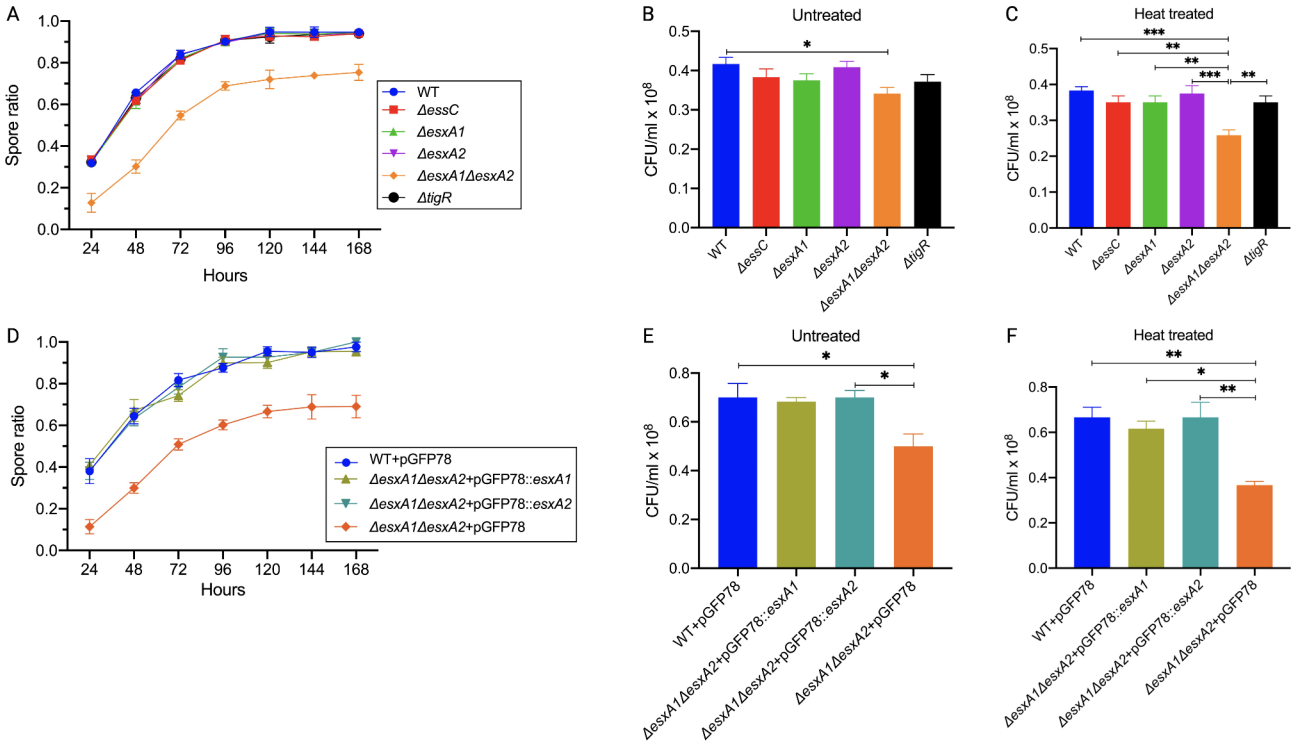

Fig. 4 Sporulation rates and spore viability of experiment strains cultured in DSM at 30 °C. **A**. Time course sporulation rates were calculated as the ratio of CFUs/ml for heat-treated and untreated WT and its mutants. The mean CFU/ml for untreated (**B**) and heat-treated (**C**) cultures obtained after 120 h of culture. **D**. Time course sporulation rates for complemented strains and their mean CFUs/ml for the untreated (**E**) and heat-treated cultures (**F**). Statistical significance was calculated using Ordinary one-way ANOVA with Dunnett's multiple comparisons test, *$P < 0.0382$; **$P < 0.0093$; ***$P < 0.006$ for three independent experiments

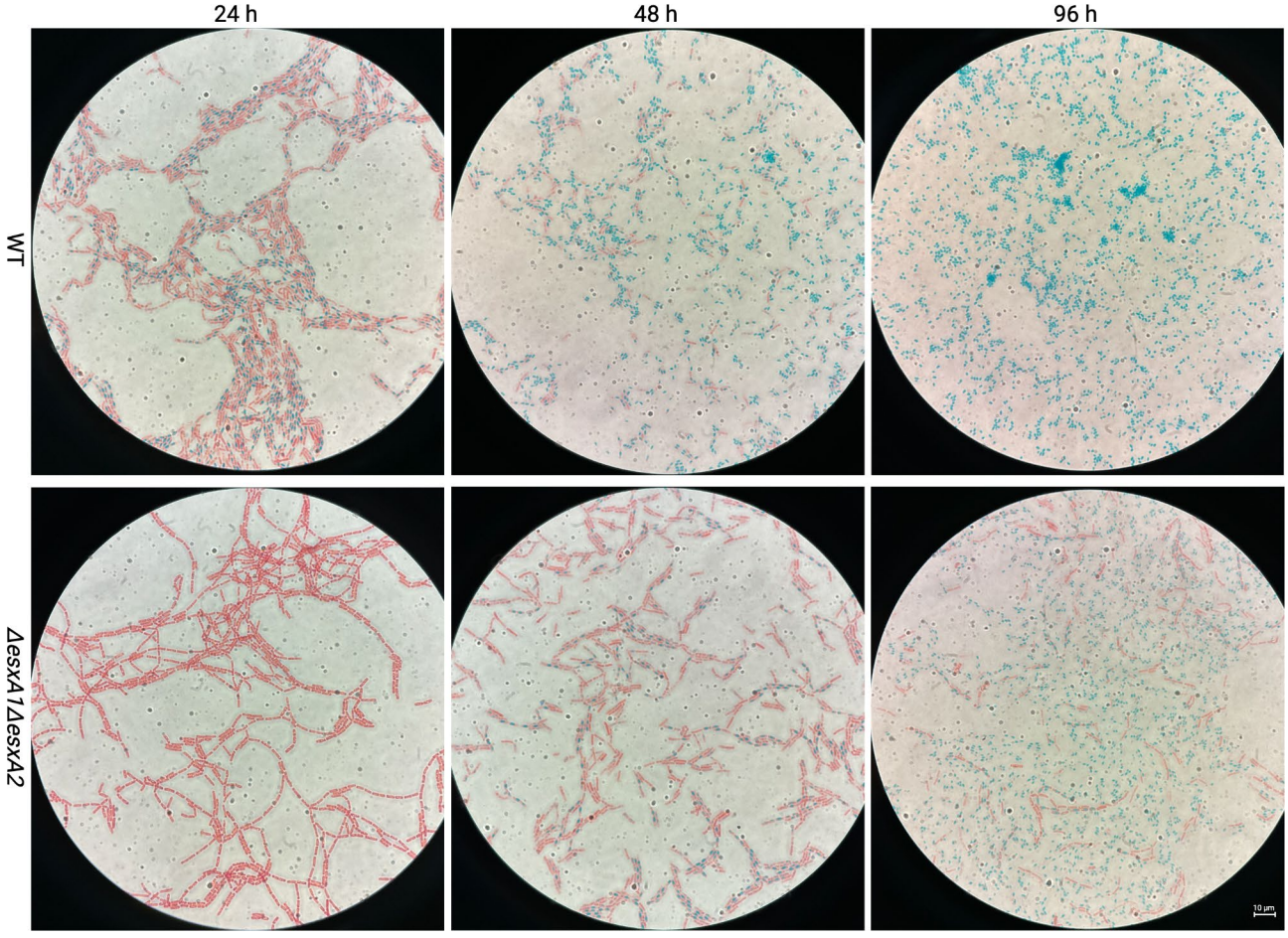

Fig. 5 The spore staining results of *B. cereus* ATCC14579 and *ΔesxA1ΔesxA2*. When stained with malachite green and safranin O, matured spores and endospores are stained blue, and vegetative cells are stained red. Within 24 h, more than 80% of the WT cells had formed endospores (blue cytoplasm), but less than 10% in *ΔesxA1ΔesxA2* cells, which are immature (forespores) and poorly take up the malachite green stain. After 48 h, the WT underwent 66% sporulation on average, while the mutant had approximately 45% endospores and 20% mature spores. Beyond 96 h, the WT had almost all cells sporulated, but *ΔesxA1ΔesxA2* still had vegetative cells (28%) occurring in chains

proteins work cooperatively and play a significant role in the optimal sporulation of *B. cereus* ATCC14579.

Discussion

The T7SS is characterized by an ATPase-driven secretion of approximately 100-residue helical proteins that contain a central WXG motif, with EsxA being the first identified T7SS substrate [46]. It is the major effector of the T7SS secretion system, essential for the virulence of pathogenic Gram-positive bacteria, such as *M. tuberculosis* and *S. aureus*. EsxA is required for the synthesis of EsxB and vise-versa, interacts with multiple cellular proteins, and stimulates several signal pathways [47–50]. This greatly increases the complexity of dissecting the precise roles of EsxA. To date, no study has focused on the functional roles of EsxA nor characterized the T7SSb in *B. cereus*.

In this study, we focused on establishing the repertoire of the T7SSb in *B. cereus* ATCC14579 and investigating the intrinsic roles of the T7SSb-dependent effector proteins. Through LC-MS/MS concatenated to a proteogenomic pipeline, we identified two EsxA proteins with 94% sequence identity in the wild-type culture supernatant and none in the *ΔessC* mutant. Protein sequence alignment showed that this pair belonged to the *sag*EsxA-like subfamily of the WXG100 superfamily. WXG100 proteins form dimeric complexes within the cytoplasm before secretion to increase solubility, and the driving force for the interdimer interactions is principally hydrophobic [42, 51]. However, a pair of conserved and hydrophilic mutations among the proteins of the *sag*EsxA-like subfamily allows for interdimer hydrogen bonding. As a result, this conserved pair of mutations is seen as a fingerprint of homodimeric WXG100 proteins, which is in tandem with our finding of two nearly identical EsxA proteins (Fig. 2B). In contrast, ESAT-6-like and EsxB found in *S. aureus* and *M. tuberculosis* form heterodimers that only possess hydrophobic residues for interdimer

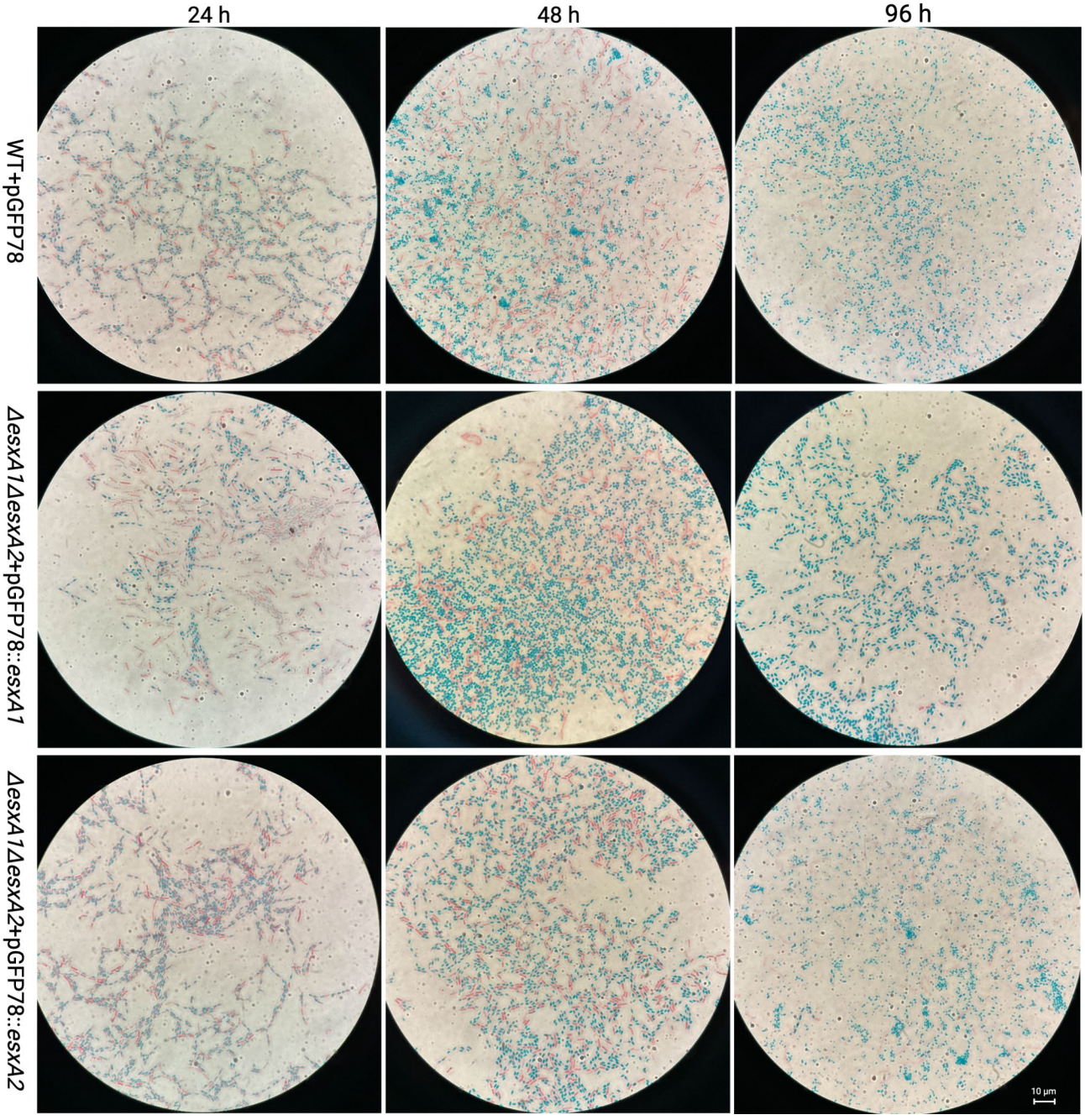

Fig. 6 The spore staining results of complementary strains. Complementation of *ΔesxA1ΔesxA2* with either pGFP78::*esxA1* or pGFP78::*esxA2* restored sporulation rates to levels of the WT. Spores and endospores are stained blue, while vegetative cells red. The WT was also complemented with pGFP78 to allow growth of all complemented strains under similar conditions in 10 µg/ml tetracycline

interaction [42]. Our genome analysis did not find an EsxB candidate, similarly, *B. subtilis* T7SS lacks the EsxB homolog (Fig. 1) [19, 20]. Among *Bacillus* species, EsxB has only been identified in *B. anthracis*, but it lacks EsxA [21]. In addition, some members of the Firmicutes group have the atypical WXG100-like proteins, EsxC and EsxD, encoded on the same operon or within the T7SS gene cluster [16]. However, in *B. cereus*, a TIGR04197 protein family gene was found downstream of the orphaned *esxA1*, sharing the same operon (Fig. 1). The protein sequence has no known signal peptide or interactions but based on the curated Hidden Markov Model-based and BLAST-based protein families, members of the TIGR04197 protein family are similar in length and sequence. Phylogenetic profiling shows that members of

this family are similarly restricted to species with T7SS, making this family a related set of T7SS effectors.

Homology analysis among *B. cereus* strains showed that the T7SSb gene cluster is conserved from the 5' end up to the proximal two-thirds of the *essC*. One-third on the 3' end of *essC* and the ensuing genes within the T7SSb cluster showed variation among the strains. This could suggest that *B. cereus* strains have different *essC* alleles, with each allele followed by a distinct set of genes. The less virulent *B. cereus* ATCC14579 and *B. cereus* BC33 did not possess virulence-encoding genes in the variable region. In contrast, the clinical isolates, *B. cereus* ST1420 and *B. cereus* B4264, possess a second TIGR04197 protein and LXG toxin genes (Fig. 1). *B. cereus* ST1420 was a major sequence type associated with nosocomial infections and bacteremia in Japan [2], while *B. cereus* B4264 was isolated from a case of fatal pneumonia in a male patient cultured from the blood and the pleural fluid in the USA [52]. The variable 3' end of the *essC* encodes the C-terminal ATPase domain to which the substrate binds before secretion. The EssC variants among Firmicutes are associated with unique effector repertoires, it is likely that a given EssC may only export substrates encoded by their cognate subtype. Studies on T7SSb in *S. aureus* and *Listeria monocytogenes* strains have identified multiple *essC* alleles defined by downstream substrates. *S. aureus* and *L. monocytogenes* strains have been grouped into four and seven T7SSb variants, respectively [16, 53, 54]. *S. aureus* strains with *essC1* are clinical isolates, possessing *esxA*, *esxB*, *esxC*, *esxD*, and an LXG toxin gene followed by immunity genes, while the less pathogenic strains with *essC2* and *essC3*, the *esxD* is replaced by *tigR* [16, 53]. TIGR04197 could play a significant role, yet to be known, in the T7SSb function. Our findings, and those of others, show that the T7SSb is very diverse between and within species, a reflection of virulence and implications for varied functions among the Firmicutes group.

Recent studies on T7SS continue to focus on its involvement in host-immune interactions and niche adaptations, which are diverse given the inter and intra-species variations in the repertoire. We also need to start unraveling the intrinsic roles of the T7SS, which could provide insights into the pathways they are involved in and serve as new targets for antimicrobials in the wake of emerging drug-resistant bacteria [55, 56]. Here, we screened for alterations in the phenotypic characteristics that gene deletions in the secretion system might cause in *B. cereus* ATCC14579. We found colony size and morphology, hemolytic and proteolytic activities, and growth kinetics similar to the wild type. When tested for sporulation in DSM, we found that the strain lacking both *esxA* genes, *ΔesxA1ΔesxA2*, had a delayed and significantly reduced ability to form spores. It was evident from the spore ratio that *ΔesxA1ΔesxA2* had significantly fewer viable spores throughout the culture period compared to the WT and other mutants (Fig. 4). Generally, a higher bacterial culture optical density is assumed to translate to a higher CFU count, however, our findings for the *ΔesxA1ΔesxA2* defied that notion. Phase contrast microscopy showed no evident aberrations in cell and spore morphologies, only a delayed and reduced sporulation in *ΔesxA1ΔesxA2*, which agreed with the CFU results. Overall, the *ΔesxA1ΔesxA2* culture still had vegetative cells reaching 28% on average of any microscopic field viewed (Fig. 5). When complemented with either *esxA1* or *esxA2*, the mutant fully recovered the spore formation ability (Fig. 6), suggesting the cooperative function of the EsxA1 and EsxA2 and their involvement in sporulation of *B. cereus*. In contrast, the *ΔessC* mutant, in which we found that EsxA was not secreted, had similar sporulation results as the WT. This indicated that EsxA did not affect sporulation after being secreted, but its expression within the cell was necessary to maintain optimum sporulation. Thus, *ΔesxA1*, *ΔesxA2*, and *ΔtigR* sporulation phenotypes were unaffected. These findings confirmed that EsxA is not only a secreted effector protein but has additional roles within the milieu and, in this case, sporulation. Other studies have also indicated that T7SS-dependent effectors have other roles within the bacterium. Fyans *et al*. [57] reported that the ESX/type VII secretion system modulated development but not virulence in *Streptomyces scabies*, a plant pathogen. Specifically, the EsxA and EsxB mutants had abnormal spore chains and exhibited resistance to lysis by the *Streptomyces*-specific phage ϕC31. Similarly, deletion of the EsxAB operon in *Streptomyces coelicolor* resulted in irregular-sized pre-spore compartments with corresponding aberrant DNA contents. The EsxAB heterodimer was proposed to control the coordination of cell division with the segregation of nucleoids, most probably through interaction with other factors that regulate nucleoid condensation [58]. However, in *B. cereus*, growth, size, and morphology of the colonies and cells of the *ΔesxA1ΔesxA2* mutant were unaffected. The T7SS-mediated phenotypes seemingly depend on T7SS subtype-specific regulation and secreted effectors, a pandora's box yet to be opened. Thus, T7SS substrates possess diverse species-specific cellular functions and can modulate interactions between bacteria and eukaryotic cells [44, 47, 49].

One possible mechanism of how EsxA plays an important role in the sporulation in *B. cereus* is that EsxA may interact with SpoIIIE and enhance its functionality. The protein-protein interaction analysis using STRING [59] (https://string-db.org) showed that YukE, an EsxA from *B. subtilis*, may interact with SpoIIIE (Fig. S4A). SpoIIIE is a DNA translocase that drives up to 70% of the chromosome across the forespore septum before endospore formation [60, 61]. Since *B. cereus* EsxA proteins were

unable to be analyzed in the STRING database, and the sporulation pathway is well understood in *B. subtilis* [62–65], the prediction data was obtained using *B. subtilis* protein information. Although the amino acid sequences of EsxA and YukE have low homology, the superimposition of their predicted structures was nearly perfect (Fig.S4B). Further, the SpoIIIE proteins from *B. cereus* and *B. subtilis* were predicted to possess a high structural homology (Fig. S4C), therefore, we speculate that EsxA-SpoIIIE interaction may occur, and it impact sporulation in *B. cereus.* In addition, we also found that the ATPase domain of *B. cereus* SpoIIIE had a high structural similarity with the ATPase domain of EssC protein, as Mietrach *et al*. revealed previously [66]. Just like EsxB binds to EssC, causing the multimerization of EssC to form the hexameric secretion pore [24, 67], SpoIIIE also forms a hexameric pore to pass DNA [13, 23]. Hence, in the absence of EsxB in *B. cereus* ATCC14679, we conjecture that EsxA may promote EssC and SpoIIIE multimerization. Previously, it was observed in *S. coelicolor* that the loss of function of the EsxAB heterodimer impacted the coordination of cell division and the segregation of nucleoids. But even multiple gene mutations involved in the coordination of nucleoid condensation and segregation, including *ftsK*, also resulted in similar septation aberrations, implying it depends on several overlapping and partially redundant functions [58]. Similarly, in *B. cereus* ATCC14579, loss of EsxA1 and EsxA2 may be impacting the sporulation function of SpoIIIE, an FtsK protein. Thus, without EsxA in the *ΔesxA1ΔesxA2* mutant, SpoIIIE translocation of chromosomal DNA may have been inefficient, resulting in delayed sporulation and fewer mature spores in *B. cereus* ATCC14579. On the other hand, EsxA might have a completely different novel mechanism affecting sporulation, which regulates the function or transcription of sporulation-related genes. The detailed molecular mechanisms of how EsxA regulates *B. cereus* sporulation and its biological significance in the *B. cereus* lifecycles, including the virulence, need to be addressed in future studies.

Conclusion

B. cereus T7SSb possesses a pair of nearly identical effector proteins named EsxA belonging to the *sag*EsxA-like subfamily of the WXG100 protein superfamily. Single gene mutations in the T7SSb effectors and core machinery did not alter the growth characteristics of *B. cereus* ATCC14579. However, deletion of the two *esxA* genes resulted in a significantly delayed sporulation and fewer viable spores/ml in a sporulation-inducing culture. Additionally, complementation of the *ΔesxA1ΔesxA2* mutant with a single *esxA* gene was sufficient to recover maximum sporulation ability. Altogether, these results consistently showed that EsxA is essential for spore formation in *B. cereus* ATCC14579, a novel finding for a T7SSb-dependent effector molecule.

Supplementary Information

The online version contains supplementary material available at https://doi.org/10.1186/s12866-024-03492-1.

Supplementary Material 1

Supplementary Material 2

Acknowledgements

We thank the Open Facility, Global Facility Center, Creative Research Institution, Hokkaido University for allowing us to conduct the analysis of peptide mixture using the HPLC and Hybrid Ion Trap-Orbitrap Mass Spectrometer, which greatly assisted the research. We are grateful to Yunrong Chai and Yinghao He (Northeastern University, Boston) for generously providing the pGFP78 DNA.

Author contributions

H.K.K. and H.H. conceptualized the study. H.K.K., A.P. and Y.F. designed the experiments. H.K.K., M.Su. and Y.F. carried out the experiments. H.K.K., M.Sh., J.Y.C., T.Z. and T.K. contributed to data analysis and interpretation of results. H.K.K., A.P., and M.Sh. drafted the manuscript, while Y.F., M.M., B.M.H., T.K. and A.P. reviewed and edited it. H.H. and A.P. supervised the study. All authors read and approved the final manuscript.

Funding

This work was supported by the Ministry of Education, Culture, Sports, Science and Technology (MEXT) in Japan or Japan Society for the Promotion of Science under Grants-in-Aid for Scientific Research (KAKENHI) to H.H. (Grant No.17H01679 and 18K19436) and A.P. (Grant No. 19K16653 and 21K15430), World-leading Innovative and Smart Education (WISE) Grant-in-Aid for Graduate Students to H.K.K., and the Japan International Cooperation Agency (JICA) scholarship for Advanced Training Program for Fostering Global Leaders on Infectious Disease Control to Build Resilience against Public Health Emergencies to H.K.K.

Data availability

The *B. cereus* (ATCC14579, BC33, B4262, and ST1420), *S. aureus* USA300, and *B. subtilis* 168 genome datasets used in the analysis of the type VIIb secretion system were downloaded from NCBI Genome under the GenBank file numbers NC_004722.1, CP072774.1, CP001176.1, AP022975.1, CP092052.1, and AL009126.3 respectively.

Declarations

Ethics approval and consent to participate

Not applicable.

Consent for publication

Not applicable.

Competing interests

The authors declare no competing interests.

Author details

[1]Division of Infection and Immunity, International Institute for Zoonosis Control, Hokkaido University, Sapporo, Japan
[2]GenEndeavor LLC, 26219 Eden Landing Rd, Hayward, CA 94545, USA
[3]Hokudai Center for Zoonosis Control in Zambia, University of Zambia, Lusaka, Zambia
[4]International Collaboration Unit, International Institute for Zoonosis Control, Hokkaido University, Sapporo, Japan
[5]Zambia National Public Health Institute, Ministry of Health, Lusaka, Zambia
[6]Microbiology Unit, Paraclinical Studies, School of Veterinary Medicine, University of Zambia, Lusaka, Zambia

[7]Public Health Unit, Disease Control Studies, School of Veterinary Medicine, University of Zambia, Lusaka, Zambia

Received: 11 January 2024 / Accepted: 3 September 2024
Published online: 17 September 2024

References

1. Acosta Pedemonte NB, Rocchetti NS, Villalba J, Lerman Tenenbaum D, Settecase CJ, Bagilet DH, et al. *Bacillus cereus* bacteremia in a patient with an abdominal stab wound. Rev Argent Microbiol. 2020;52(2):115–7.
2. Akamatsu R, Suzuki M, Okinaka K, Sasahara T, Yamane K, Suzuki S, et al. Novel sequence type in *Bacillus cereus* strains associated with nosocomial infections and bacteremia, Japan. Emerg Infect Dis. 2019;25(5):883–90.
3. Klee SR, Ozel M, Appel B, Boesch C, Ellerbrok H, Jacob D, et al. Characterization of *Bacillus anthracis*-like bacteria isolated from wild great apes from Cote d'Ivoire and Cameroon. J Bacteriol. 2006;188(15):5333–44.
4. Enosi Tuipulotu D, Mathur A, Ngo C, Man SM. *Bacillus cereus*: epidemiology, virulence factors, and host–Pathogen interactions. Trends Microbiol. 2021;29(5):458–71.
5. Abdallah AM, van Gey NC, Champion PAD, Cox J, Luirink J, Vandenbroucke-Grauls CMJE, et al. Type VII secretion–mycobacteria show the way. Nat Rev Microbiol. 2007;5(11):883–91.
6. Bunduc CM, Bitter W, Houben ENG. Structure and function of the mycobacterial type VII Secretion systems. Annu Rev Microbiol. 2020;74(1):315–35.
7. Kneuper H, Cao ZP, Twomey KB, Zoltner M, Jäger F, Cargill JS, et al. Heterogeneity in *ess* transcriptional organization and variable contribution of the Ess/Type VII protein secretion system to virulence across closely related *Staphylococcus aureus* strains. Mol Microbiol. 2014;93(5):928–43.
8. Spencer BL, Tak U, Mendonça JC, Nagao PE, Niederweis M, Doran KS. A type VII secretion system in Group B *Streptococcus* mediates cytotoxicity and virulence. PLoS Pathog. 2021;17(12):e1010121.
9. Pym AS, Brodin P, Brosch R, Huerre M, Cole ST. Loss of RD1 contributed to the attenuation of the live tuberculosis vaccines *Mycobacterium bovis* BCG and *Mycobacterium microti*. Mol Microbiol. 2002;46(3):709–17.
10. Smith J, Manoranjan J, Pan M, Bohsali A, Xu J, Liu J, et al. Evidence for pore formation in host cell membranes by ESX-1-Secreted ESAT-6 and its role in *Mycobacterium marinum* escape from the Vacuole. Infect Immun. 2008;76(12):5478–87.
11. Tak U, Dokland T, Niederweis M. Pore-forming esx proteins mediate toxin secretion by *Mycobacterium tuberculosis*. Nat Commun. 2021;12(1):394.
12. Cao Z, Casabona MG, Kneuper H, Chalmers JD, Palmer T. The type VII secretion system of *Staphylococcus aureus* secretes a nuclease toxin that targets competitor bacteria. Nat Microbiol. 2016;2(1):16183.
13. Chan H, Mohamed AMT, Grainge I, Rodrigues CDA. FtsK and SpoIIIE, coordinators of chromosome segregation and envelope remodeling in bacteria. Trends Microbiol. 2022;30(5):480–94.
14. Callahan B, Nguyen K, Collins A, Valdes K, Caplow M, Crossman DK, et al. Conservation of structure and protein-protein interactions mediated by the secreted mycobacterial proteins EsxA, EsxB, and EspA. J Bacteriol. 2010;192(1):326–35.
15. Champion PAD, Stanley SA, Champion MM, Brown EJ, Cox JS. C-Terminal Signal sequence promotes virulence factor secretion in Mycobacterium tuberculosis. Sci (1979). 2006;313(5793):1632–6.
16. Warne B, Harkins CP, Harris SR, Vatsiou A, Stanley-Wall N, Parkhill J, et al. The Ess/Type VII secretion system of *Staphylococcus aureus* shows unexpected genetic diversity. BMC Genomics. 2016;17(1):222.
17. Bobrovskyy M, Chen X, Missiakas D. The type 7b secretion system of *S. Aureus* and its role in colonization and systemic infection. Infect Immun. 2023;91(5).
18. Klein TA, Grebenc DW, Shah PY, McArthur OD, Dickson BH, Surette MG et al. Dual targeting factors are required for LXG Toxin Export by the bacterial type VIIb secretion system. mBio. 2022;13(5).
19. Tassinari M, Doan T, Bellinzoni M, Chabalier M, Ben-Assaya M, Martinez M et al. The antibacterial type VII secretion system of *Bacillus subtilis*: structure and interactions of the pseudokinase YukC/EssB. mBio. 2022;13(5).
20. Huppert LA, Ramsdell TL, Chase MR, Sarracino DA, Fortune SM, Burton BM. The ESX System in *Bacillus subtilis* mediates protein secretion. PLoS ONE. 2014;9(5):e96267.
21. Garufi G, Butler E, Missiakas D. ESAT-6-Like protein secretion in *Bacillus anthracis*. J Bacteriol. 2008;190(21):7004–11.
22. Fleming TC, Shin JY, Lee SH, Becker E, Huang KC, Bustamante C, et al. Dynamic SpoIIIE assembly mediates septal membrane fission during *Bacillus subtilis* sporulation. Genes Dev. 2010;24(11):1160–72.
23. Fiche JB, Cattoni DI, Diekmann N, Langerak JM, Clerte C, Royer CA, et al. Recruitment, Assembly, and Molecular Architecture of the SpoIIIE DNA pump revealed by Superresolution Microscopy. PLoS Biol. 2013;11(5):e1001557.
24. Rosenberg OS, Dovala D, Li X, Connolly L, Bendebury A, Finer-Moore J, et al. Substrates control multimerization and activation of the multi-domain ATPase motor of type VII secretion. Cell. 2015;161(3):501–12.
25. Nicholson WL, Setlow P, Harwood C, Cutting SM. Molecular biological methods for *Bacillus*. New York, USA: John Willey; 1990. pp. 391–450.
26. Plaut RD, Stibitz S. Improvements to a markerless allelic exchange system for *Bacillus anthracis*. PLoS ONE. 2015;10(12):e0142758.
27. Gao T, Foulston L, Chai Y, Wang Q, Losick R. Alternative modes of biofilm formation by plant-associated *Bacillus cereus*. Microbiologyopen. 2015;4(3):452–64.
28. Ivanova N, Sorokin A, Anderson I, Galleron N, Candelon B, Kapatral V, et al. Genome sequence of *Bacillus cereus* and comparative analysis with *Bacillus anthracis*. Nature. 2003;423(6935):87–91.
29. Simon R, Priefer U, Pühler A. A Broad Host Range Mobilization System for in Vivo Genetic Engineering: Transposon Mutagenesis in Gram negative Bacteria. Bio/Technology. 1983;1(9):784–91.
30. Chan QWT, Howes CG, Foster LJ. Quantitative Comparison of Caste Differences in Honeybee Hemolymph. Mol Cell Proteom. 2006;5(12):2252–62.
31. Deng W, Yu HB, de Hoog CL, Stoynov N, Li Y, Foster LJ, et al. Quantitative proteomic analysis of type III secretome of Enteropathogenic *Escherichia coli* reveals an expanded Effector Repertoire for Attaching/Effacing bacterial pathogens. Cell Proteom. 2012;11(9):692–709. Molecular.
32. Qian C, Chen H, Johs A, Lu X, An J, Pierce EM, et al. Quantitative proteomic analysis of biological processes and responses of the Bacterium *Desulfovibrio desulfuricans* ND132 upon deletion of its Mercury methylation genes. Proteomics. 2018;18(17):1700479.
33. Kanehisa M. Linking databases and organisms: GenomeNet resources in Japan. Trends Biochem Sci. 1997;22(11):442–4.
34. Altschul SF, Gish W, Miller W, Myers EW, Lipman DJ. Basic local alignment search tool. J Mol Biol. 1990;215(3):403–10.
35. Guy L, Roat Kultima J, Andersson SGE. genoPlotR: comparative gene and genome visualization in R. Bioinformatics. 2010;26(18):2334–5.
36. Li L, Jin J, Hu H, Deveau IF, Foley SL, Chen H. Optimization of sporulation and purification methods for sporicidal efficacy assessment on *Bacillus* spores. J Ind Microbiol Biotechnol. 2022;49(4).
37. Huang Q, Zhang Z, Liu Q, Liu F, Liu Y, Zhang J, et al. SpoVG is an important regulator of sporulation and affects biofilm formation by regulating Spo0A transcription in *Bacillus cereus*. BMC Microbiol. 2021;21(1):0–9.
38. Nicholson WL, Schuerger AC. *Bacillus subtilis* spore survival and expression of Germination-Induced Bioluminescence after prolonged incubation under simulated Mars Atmospheric pressure and composition: implications for Planetary Protection and Lithopanspermia. Astrobiology. 2005;5(4):536–44.
39. Oktari A, Supriatin Y, Kamal M, Syafrullah H. The bacterial endospore stain on Schaeffer Fulton using variation of Methylene Blue Solution. J Phys Conf Ser. 2017;812:012066.
40. Ulhuq FR, Gomes MC, Duggan GM, Guo M, Mendonca C, Buchanan G, et al. A membrane-depolarizing toxin substrate of the Staphylococcus aureus type VII secretion system mediates intraspecies competition. Proc Natl Acad Sci. 2020;117(34):20836–47.
41. Kobayashi K. Diverse LXG toxin and antitoxin systems specifically mediate intraspecies competition in *Bacillus subtilis* biofilms. PLoS Genet. 2021;17(7):e1009682.
42. Poulsen C, Panjikar S, Holton SJ, Wilmanns M, Song YH. WXG100 protein superfamily consists of three subfamilies and exhibits an α-Helical C-Terminal conserved Residue Pattern. PLoS ONE. 2014;9(2):e89313.
43. Sysoeva TA, Zepeda-Rivera MA, Huppert LA, Burton BM. Dimer recognition and secretion by the ESX secretion system in *Bacillus subtilis*. Proceedings of the National Academy of Sciences. 2014;111(21):7653–8.
44. Spencer BL, Doran KS. Evolving understanding of the type VII secretion system in Gram-positive bacteria. PLoS Pathog. 2022;18(7):e1010680.
45. Flint JL, Kowalski JC, Karnati PK, Derbyshire KM. The RD1 virulence locus of *Mycobacterium tuberculosis* regulates DNA transfer in *Mycobacterium smegmatis*. Proceedings of the National Academy of Sciences. 2004;101(34):12598–603.

46. Unnikrishnan M, Constantinidou C, Palmer T, Pallen MJ. The enigmatic esx proteins: looking Beyond Mycobacteria. Trends Microbiol. 2017;25(3):192–204.
47. Burts ML, Williams WA, DeBord K, Missiakas DM. EsxA and EsxB are secreted by an ESAT-6-like system that is required for the pathogenesis of Staphylococcus aureus infections. Proc Natl Acad Sci. 2005;102(4):1169–74.
48. Korea CG, Balsamo G, Pezzicoli A, Merakou C, Tavarini S, Bagnoli F, et al. Staphylococcal esx proteins modulate apoptosis and release of Intracellular *Staphylococcus aureus* during infection in epithelial cells. Infect Immun. 2014;82(10):4144–53.
49. Zhang Q, Wang D, Jiang G, Liu W, Deng Q, Li X, et al. EsxA membrane-permeabilizing activity plays a key role in mycobacterial cytosolic translocation and virulence: effects of single-residue mutations at glutamine 5. Sci Rep. 2016;6(1):32618.
50. Bao Y, Wang L, Sun J. A small protein but with diverse roles: a review of EsxA in *Mycobacterium*–host Interaction. Cells. 2021;10(7):1645.
51. Renshaw PS, Panagiotidou P, Whelan A, Gordon SV, Hewinson RG, Williamson RA, et al. Conclusive evidence that the major T-cell antigens of the *Mycobacterium tuberculosis* Complex ESAT-6 and CFP-10 form a tight, 1:1 complex and characterization of the Structural properties of ESAT-6, CFP-10, and the ESAT-6·CFP-10 complex. J Biol Chem. 2002;277(24):21598–603.
52. Dodson RJ, Durkin AS, Rosovitz MJ, Rasko DA, Hoffmaster A, Ravel J et al. Genome sequence of *Bacillus cereus* B4264. Vol. Direct sub, NCBI. Maryland; 2008.
53. Bowman L, Palmer T. The type VII secretion system of *Staphylococcus*. Annu Rev Microbiol. 2021;75(1):471–94.
54. Bowran K, Palmer T. Extreme genetic diversity in the type VII secretion system of *Listeria monocytogenes* suggests a role in bacterial antagonism. Microbiol (N Y). 2021;167(3).
55. Baron C, Coombes B. Targeting bacterial Secretion systems: benefits of disarmament in the Microcosm. Infect Disord Drug Targets. 2007;7(1):19–27.
56. Belete TM. Novel targets to develop new antibacterial agents and novel alternatives to antibacterial agents. Hum Microb J. 2019;11:100052.
57. Fyans JK, Bignell D, Loria R, Toth I, Palmer T. The ESX type VII secretion system modulates development, but not virulence, of the plant pathogen *Streptomyces scabies*. Mol Plant Pathol. 2013;14(2):119–30.
58. Akpe San Roman S, Facey PD, Fernandez-Martinez L, Rodriguez C, Vallin C, Del Sol R, et al. A heterodimer of EsxA and EsxB is involved in sporulation and is secreted by a type VII secretion system in *Streptomyces coelicolor*. Microbiol (N Y). 2010;156(6):1719–29.
59. Szklarczyk D, Kirsch R, Koutrouli M, Nastou K, Mehryary F, Hachilif R, et al. The STRING database in 2023: protein–protein association networks and functional enrichment analyses for any sequenced genome of interest. Nucleic Acids Res. 2023;51(D1):D638–46.
60. Wu LJ, Lewis PJ, Allmansberger R, Hauser PM, Errington J. A conjugation-like mechanism for prespore chromosome partitioning during sporulation in *Bacillus subtilis*. Genes Dev. 1995;9(11):1316–26.
61. Wu LJ, Errington J. Bacillus subtilis spoIIIE protein required for DNA segregation during Asymmetric Cell Division. Sci (1979). 1994;264(5158):572–5.
62. Eijlander RT, de Jong A, Krawczyk AO, Holsappel S, Kuipers OP. SporeWeb: an interactive journey through the complete sporulation cycle of *Bacillus subtilis*. Nucleic Acids Res. 2014;42(D1):D685–91.
63. Higgins D, Dworkin J. Recent progress in *Bacillus subtilis* sporulation. FEMS Microbiol Rev. 2012;36(1):131–48.
64. Riley EP, Schwarz C, Derman AI, Lopez-Garrido J. Milestones in *Bacillus subtilis* sporulation research. Microb Cell. 2021;8(1):1–16.
65. Omony J, de Jong A, Krawczyk AO, Eijlander RT, Kuipers OP. Dynamic sporulation gene co-expression networks for *Bacillus subtilis* 168 and the food-borne isolate *Bacillus amyloliquefaciens*: a transcriptomic model. Microb Genom. 2018;4(2).
66. Mietrach N, Damián-Aparicio D, Mielich-Süss B, Lopez D, Geibel S. Substrate Interaction with the EssC coupling protein of the type VIIb secretion system. J Bacteriol. 2020;202(7).
67. Bobrovskyy M, Oh SY, Missiakas D. Contribution of the EssC ATPase to the assembly of the type 7b secretion system in *Staphylococcus aureus*. J Biol Chem. 2022;298(9):102318.

Publisher's note